

# NJC

Accepted Manuscript



This is an *Accepted Manuscript*, which has been through the Royal Society of Chemistry peer review process and has been accepted for publication.

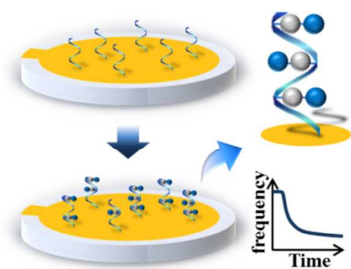
*Accepted Manuscripts* are published online shortly after acceptance, before technical editing, formatting and proof reading. Using this free service, authors can make their results available to the community, in citable form, before we publish the edited article. We will replace this *Accepted Manuscript* with the edited and formatted *Advance Article* as soon as it is available.

You can find more information about *Accepted Manuscripts* in the [Information for Authors](#).

Please note that technical editing may introduce minor changes to the text and/or graphics, which may alter content. The journal's standard [Terms & Conditions](#) and the [Ethical guidelines](#) still apply. In no event shall the Royal Society of Chemistry be held responsible for any errors or omissions in this *Accepted Manuscript* or any consequences arising from the use of any information it contains.



[www.rsc.org/njc](http://www.rsc.org/njc)



- ▶ Label-free, ultra-sensitive and in-situ detection of silver ion was achieved using quartz crystal microbalance in laboratory and drinking water condition

**Ultra-sensitive in situ detection of silver ions using quartz crystal microbalance**

Sangmyung Lee,<sup>†,#</sup>Kuewhan Jang,<sup>†,#</sup>Chanho Park,<sup>†</sup>Juneseok You,<sup>†</sup>Taegyung

Kim,<sup>‡</sup>ChulhwanIm,<sup>‡</sup>Junoh Kang,<sup>‡</sup>Haneul Shin,<sup>‡</sup> Chang-Hwan Choi,<sup>§</sup>Jinsung Park,<sup>⊥,\*</sup>Sungsoo

Na<sup>†,\*</sup>

<sup>†</sup>Department of Mechanical Engineering, Korea University, Seoul 136-701, Republic of

Korea

<sup>\*</sup>The School for Gifted Students Seoul Science High School, Seoul 110-530, Republic of

Korea

<sup>§</sup>Department of Mechanical Engineering, Stevens Institute of Technology, Hoboken, New

Jersey 07030, USA

<sup>⊥</sup>Department of Control and Instrumentation Engineering, Korea University, Jochiwon 339-

700, Republic of Korea

<sup>\*</sup>Corresponding author

E-mail address: nanojspark@gmail.com(J. Park), nass@korea.ac.kr (S. Na)

<sup>#</sup>These authors contributed equally to this work

**ABSTRACT**

Detection of toxic nanomaterials is highly important, as their scientific and engineering applications have rapidly increased recently. Consequently, they can harmfully impact human health and environment. Herein, we report the quartz crystal microbalance (QCM)-based, in situ and real-time detection of toxic silver ions by frequency shift. Generally, silver ions are so small that they are difficult to identify by using conventional microscopy. However, by using QCM and a label-free silver-specific cytosine DNA, ultra-sensitive in situ detection of silver ions is performed. The Limit of Detection (LOD) of this sensor platform is 100pM which is ten times lower than previous cantilever work. It also detects silver ions rapidly in real time which is done within 10 min. Furthermore, our proposed detection method is able to detect in drinking water. The results suggest that QCM-based detection opens a new avenue for the development of a practical water-testing sensor.

**Keywords**

Silver ion ( $\text{Ag}^+$ ), Detection, Quartz crystal microbalance (QCM), Label-free, In-situ, Cytosine

**1. Introduction**

During the last decades, scientific research and industrial innovations of nanomaterials have made dramatic advancements. Especially silver ions ( $\text{Ag}^+$ ) and silver nanoparticles have gained significant interest due to excellent properties of antimicrobial resistance and stability, enabling them to be extensively used as antimicrobial agents in many household goods such

as toothpaste and washing machines<sup>1</sup>. In addition, silver nitrates ( $\text{AgNO}_3$ ) at low concentrations have been used for the activation of bacteria *in vivo*<sup>2</sup>.  $\text{Ag}^+$  has been used not only in biological and medical fields for drug delivery, but also in many industrial areas such as photography and electronics<sup>3-5</sup>. Therefore, its global industrial waste has rapidly reached to 2500 tons per year, among which 150 tons are discarded in the form of sludge and 80 tons are emitted into the surface waters<sup>6</sup>.

As a large amount of toxic silver nanomaterials are consumed, their releases to the environment and potential impact on human health have to be concerned because cytotoxicity of  $\text{Ag}^+$  was known to occur when an organism intake the  $\text{Ag}^+$  directly or indirectly<sup>7-9</sup>. Not only that, it is reported that the biological toxicity of  $\text{Ag}^+$  has an immediate effect on many organism species, including periphyton, with the  $\text{Ag}^+$  concentration as high as 1  $\mu\text{M}$ . Biological toxicity is also known to occur even at a low  $\text{Ag}^+$  concentration, when the organism expose enough time for a while<sup>10</sup>. Since human is on the top of the food chain, human has more possibility to intake a large amount of accumulated silver ions<sup>11</sup>. In order to prevent toxic effects and other potential health-related problems, the detection of  $\text{Ag}^+$  in a few minutes is very important and necessary in a way of high sensitivity and selectivity<sup>12</sup>.

When the metal ion enters the mismatched DNA base pair, an attractive force between the metal ion and DNA base pair will arise and combine them together<sup>13</sup>. The entry of  $\text{Ag}^+$  into a cytosine-only environment leads to a specific binding and the formation of cytosine- $\text{Ag}^+$ -cytosine base pairs. In specific,  $\text{Ag}^+$  binds to nitrogen atoms of cytosine pair through hydrogen bonding. Thus, many sensors were developed for the detection of  $\text{Ag}^+$ , based on the coordination chemistry<sup>12, 14-18</sup>. In detail, Wen et al. was able to detect  $\text{Ag}^+$  by using a DNA-attached graphene-based fluorescent nanoprobe, which allowed for the observation of

combined graphene oxide and DNA with a detection limit of  $5\text{nM}^{18}$ . Similarly, Ono et al. developed a FRET (Fluorescence Resonance Energy Transfer) sensor to detect  $\text{Ag}^+$  by using the cytosine- $\text{Ag}^+$ -cytosine coordination chemistry with the resolution of  $10\text{ nM}^{19}$ . Li et al. reported an  $\text{Ag}^+$  ion-mediated DNA-based fluorescent sensor (DNAzyme) for the detection of  $\text{Ag}^+$  using ultraviolet/visible (UV/Vis) absorption spectra, and this method achieved the detection limit of  $2.5\text{ nM}^{14}$ . In addition, Li et al. reported two types of colorimetric sensing methods by using DNA-based gold nanoparticles<sup>15</sup>. One was an unlabeled detection method with the detection limit of  $52\text{ nM}$ , and the other was a labeled detection method, which required complex treatments and achieved the detection limit of  $0.6\text{nM}$ . Our previous study reported the development of an oligonucleotide-immobilized oscillator for sensing silver ions<sup>17</sup>. By using silver-specific oligonucleotide, this sensor operated based on resonant frequency shift and could detect  $\text{Ag}^+$  ions at the concentration of  $1\text{ nM}$ . More recently, we also reported the use of cytosine-rich DNA to detect  $\text{Ag}^+$  ions by surface potential shift using a Kelvin probe force microscope, and this method was capable of detecting the ions at  $1\text{ nM}^{12}$ . Despite the advances in various  $\text{Ag}^+$  ion detection methods, the shortcomings and limitations of these techniques, such as ex situ detection, high operational costs, complex treatment procedures for fluorescent substances, and long detection time, greatly disturb the availability and practical usage of these  $\text{Ag}^+$  sensors.

To overcome these technical hurdles, we have developed an ultra-sensitive  $\text{Ag}^+$  detection method by using quartz crystal microbalance (QCM) and silver-specific DNAs. QCM is an in situ detection and monitoring instrument that has been spotlighted since the 1990s. QCM can monitor a mass change of several nanograms in a highly accurate way, deduced by the Sauerbrey equation<sup>20</sup> and is useful for the investigation of interfacial phenomena at a solid

and liquid junction. Although QCM shows a high accuracy for detecting the mass change in the surface of a quartz crystal, it does not offer specific information about the change of material<sup>21</sup>. QCM is an effective method for various studies, especially for the detection of polymer adsorption and biomolecular binding on a variety of quartz crystals<sup>22</sup>, CO<sub>2</sub> capture<sup>23</sup>, selective detection using ligand-receptor or antibody-antigen<sup>24, 25</sup>, and the detection of self-assembled monolayer of cysteine on gold<sup>26</sup>, and is compatible with experiments using liquid materials. Moreover, advanced studies have demonstrated the strong capability of QCM with amplifier such as gold nanoparticles and antibodies for detection of ions<sup>27-29</sup>. In this study, we propose label-free, in-situ and selective detection method based on the use of QCM for Ag<sup>+</sup> detection. With the use of this technique, ultra-sensitive detection is achieved and direct results are obtained in a short period with real-time monitoring. In addition, our proposed method is able to selectively detect Ag<sup>+</sup> and able to detect even in regular drinking water.

## 2. Experimental Section

### 2.1 Materials

Tris-ethylenediaminetetraacetic acid(EDTA) buffer solution, AgNO<sub>3</sub>, and single cytosinewere purchased from Sigma-Aldrich (St. Louis, MO). The DNAs 5'-CCC CCC CCCCCCCCCCCCCCCCCCCCCCCC CCC-3ThioMC-3' were purchased from Integrated DNA Technology (Coralville, CA, USA).

### 2.2 Preparation of Functionalized Quartz Crystal

In this experiment, 100 μM thiol-terminated silver-specific nucleotide in the sequence of 5'-CCCCCCCCCCCCCCCCCCCCCCCCCCCCCCCCCCC-3ThioMC-3' was dissolved in an aqueous Tris-EDTA buffer solution (pH 8, sterile solution of 10 mMTris-HCl and 1 mM EDTA, Bio

Basic Inc). Next, 150 ml of silver-specific nucleotide solution was placed on a quartz crystal (5 MHz, 2.5 cm dia., Gold/Cr polished, Stanford Research Systems (Sunnyvale, CA)). After a 3-h waiting period which was sufficient time for cDNA immobilization<sup>30</sup>, the quartz crystal was washed three times with triple distilled water (pH 7.6, Millipore, Bedford, MA, USA) and then subject for day to the drying process conducted in a desiccator (Bel-Art products, Scienceware, Wayne, NJ, USA) before further analysis. In our previous studies, we stored a DNA immobilized micro-cantilever based resonator for a day<sup>31, 32</sup> which verifying that DNA immobilized platform is able to be stored for at least a day. Therefore, the DNA immobilized quartz crystal was stored in a desiccator for a day. For the reusability test, as used quartz crystal was cleaned with piranha solution ( $\text{H}_2\text{SO}_4 : \text{H}_2\text{O}_2 = 1 : 2$ ), washed with distilled water and dried in the desiccator for a day. The actual drying time of the QCM electrode for detection was enough for 2 hours in desiccator, however, for a perfect dry condition we kept drying for a day. After drying process, silver-specific nucleotide solution was placed on a quartz crystal again for further use.

### 2.3 Preparation of initial buffer and detecting solution

1  $\mu\text{M}$  single cytosine in deionized (DI) water was prepared for use as the initial buffer solution. For the preparation of detection solution, various concentrations of  $\text{Ag}^+$  solutions were prepared by dissolving  $\text{AgNO}_3$  in water (1  $\mu\text{M}$ , 100 nM, 10 nM, 1 nM, 100 pM, 10 pM and 0 M (control))<sup>17, 33</sup>, and highly concentrated cytosine solution was prepared by dissolving 1 mM single cytosine in DI water. The detection solution was obtained by combining the  $\text{Ag}^+$  solution and cytosine solution at the volume ratio of 1000:1. For selective experiment, Na, Li, Ca, Zn, Mg, Fe ion solutions were prepared as the concentration of 1  $\mu\text{M}$  in DI water, by dissolving  $\text{NaCl}_2$ ,  $\text{LiNO}_3$ ,  $\text{CaN}_2\text{O}_6$ ,  $\text{Zn}(\text{NO}_3)_2$ ,  $\text{MgCl}_2$ , and  $\text{FeCl}_3$ . In case of selective

experiment in drinking water, 1  $\mu\text{M}$  of Zn and Mg ions were added to drinking water.

#### 2.4 QCM assay for $\text{Ag}^+$ detection

Silver-specific nucleotides functionalized quartz crystal was installed onto a 200–5 MHz QCM instrument (Stanford Research Systems, Sunnyvale, CA, USA). The quartz crystal was mounted to a flow cell. The inlet tube of the flow cell was connected to both of the initial solution and detection solution through a three-way tap. The initial solution was first injected into the QCM 200 chamber to stabilize the quartz crystal. After tuning the switch, the detection solution was injected into the QCM 200 chamber for the real-time in situ detection of cytosine- $\text{Ag}^+$ -cytosine combination. Both initial solution and detection solution were injected at the flow rate of 100  $\mu\text{L}/\text{min}$  using a syringe pump (New Era Pump System, Inc., Farmingdale, NY, USA)<sup>27</sup>.

### 3. Results and Discussion

We adopted the QCM method for  $\text{Ag}^+$  detection by using silver-specific DNA which is also used in our previous studies<sup>12,17</sup>. Figure 1 schematically illustrates the in-situ  $\text{Ag}^+$  detection method based on the use of QCM and resonance frequency shift. Cytosine-rich silver-specific DNA (cDNA) was first immobilized onto the gold QCM electrode. When  $\text{Ag}^+$  were bound to DNA on the QCM electrode, the total mass of QCM electrode increased, and the resonance frequency shift occurred according to the Sauerbrey equation. Since the mass of an ion is comparable to that of an atom, the mass change caused by ion binding to DNA on the quartz electrode is so small that it is practically difficult to detect the ions at low concentrations. In our study, we used  $\text{Ag}^+$ , silver-specific DNA and single cytosine to form the cytosine- $\text{Ag}^+$ -cytosine complex. The advantage of using single cytosine is the mass amplification,

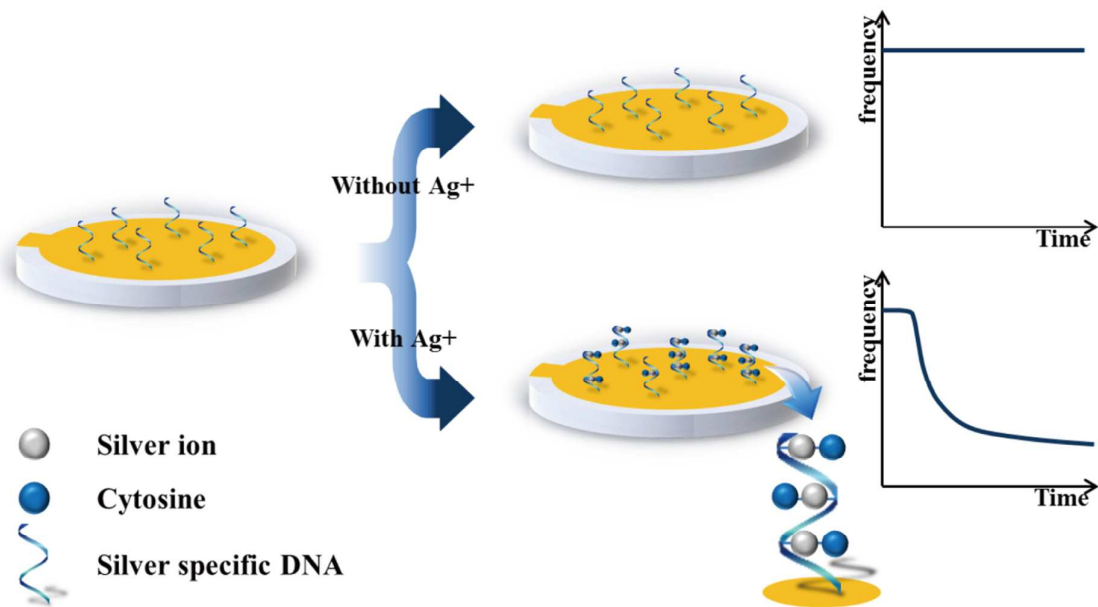


**Figure 1.** Schematic illustration of the in-situ detection of  $\text{Ag}^+$  ions by using the QCM functionalized with silver-specific DNAs and resonance frequency shift.

facilitating the sensitive detection of  $\text{Ag}^+$ . It can also prevent the formation of hairpin structure of the silver-specific DNA and enable an effective detection process.

Prior to  $\text{Ag}^+$  detection, we immobilized cDNA on the QCM electrode through thiolate-gold bonding. We performed atomic force microscopic (AFM) analysis to verify the immobilization of cDNA on the electrode. Figure 2(a) and (b) illustrate AFM images of the bare QCM electrode and cDNA-immobilized electrode. The use of AFM analysis revealed the surface roughness of each electrode (Figure 2(a) and (b)). The surface roughness of bare electrode and cDNA-immobilized electrode was  $1.0 \pm 0.0$  and  $1.7 \pm 0.1$  nm, respectively (Figure 2(d)). The increase in surface roughness was caused by the immobilization of cDNA on the electrode and significant small value of error range was the evidence of consistency of crystals. In addition, we monitored the frequency shift due to cDNA immobilization by using

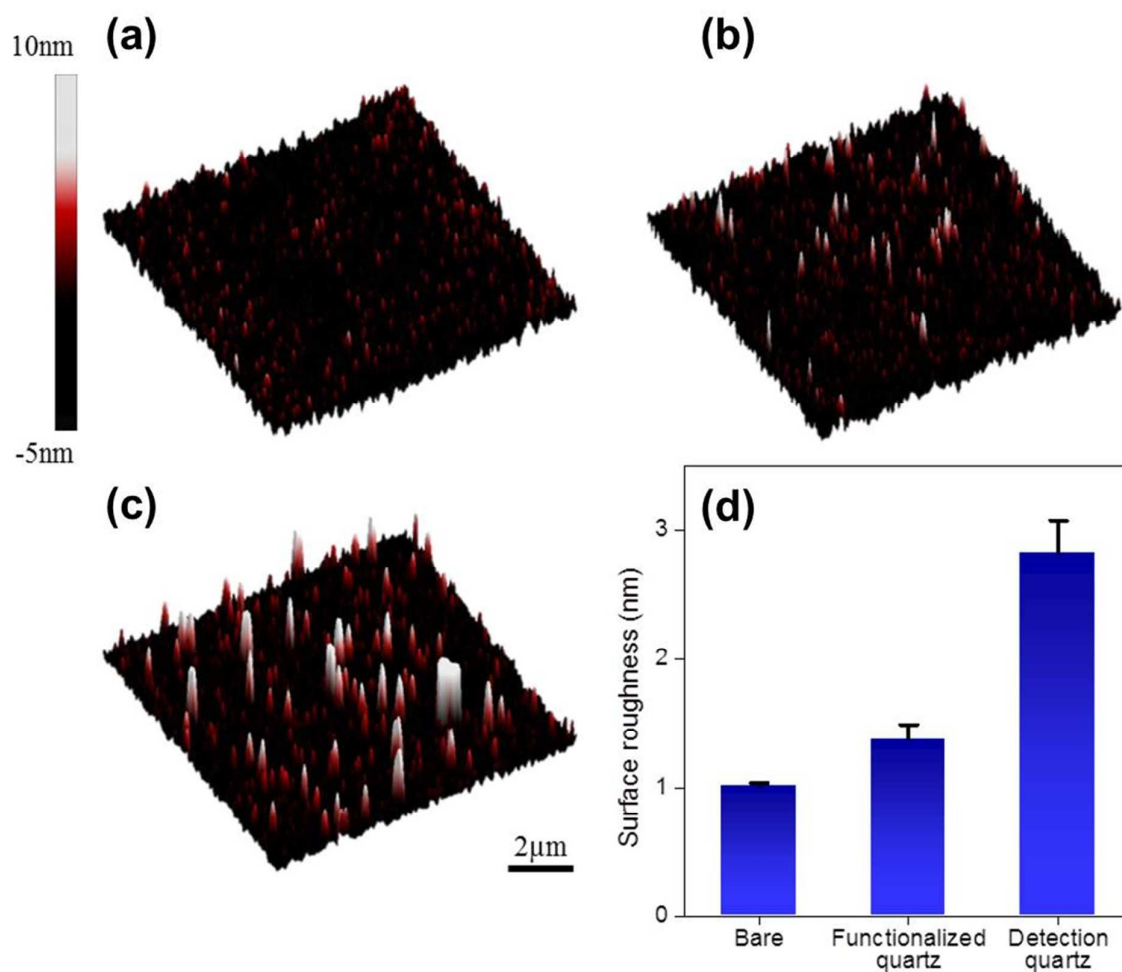


**Figure 2.** AFM images of quartz crystal in bare state (A), functionalized silver-specific state (B), and after the detection of Ag<sup>+</sup> ions (C). (D) Surface roughness(RMS) of the electrode at different states. For the statistical data, we measured AFM images from 10 different samples for each state. The error bar indicates the standard deviation. The concentration of Ag<sup>+</sup> was 1  $\mu$ M.

QCM. As the frequency shift is proportional to the increase in mass, it will occur upon the binding of cDNA to the electrode. Figure S1 shows the real-time frequency shift of cDNA immobilization with respect to time. No frequency shift was observed when the electrode was

exposed to DI water. However, when the electrode was exposed to the cDNA solution (1  $\mu\text{M}$ ), the frequency shift continuously increased and reached to 13.3 and 20.2 Hz after immobilization for 30 min and 1 hour. The results from both AFM analysis and QCM measurements indicated that cDNA was consistently immobilized on the QCM electrode (Figure S2).

After the confirmation of cDNA immobilization, we mounted the cDNA-immobilized electrode on the QCM equipment and performed  $\text{Ag}^+$  detection experiments by monitoring the frequency shift. We prepared 1  $\mu\text{M}$ , 100 nM, 10 nM, 1 nM, 100 pM, 10 pM and 0 M (control)  $\text{Ag}^+$  solutions and brought them into contact with the electrode to evaluate the sensitivity of the technique. In addition, 1  $\mu\text{M}$  cytosine was added into each  $\text{Ag}^+$  solution in order to form the cytosine- $\text{Ag}^+$ -cytosine complex. No frequency shift was observed when the electrode was exposed to the control solution (DI water and 1  $\mu\text{M}$  cytosine solution, Figure 3(a)). As expected, pronounced frequency shifts were observed when the electrode was exposed to the  $\text{Ag}^+$  solutions (Figure 3(a)). As shown in the graph, the magnitude of frequency shift increased continuously with time, and larger frequency shift values were observed at higher  $\text{Ag}^+$  concentrations. In addition, we conducted similar AFM analysis to that used for analyzing cDNA immobilization to confirm the  $\text{Ag}^+$  detection ability of the electrode. After the detection of  $\text{Ag}^+$ , the surface roughness of the cDNA-immobilized electrode increased from  $1.7 \pm 0.1$  nm to  $2.8 \pm 0.2$  nm due to the binding of  $\text{Ag}^+$  and cytosine (Figure 2(c)).

To further verify the obtained results, we analyzed the frequency shift about 30 min after the exposure of the electrode to the  $\text{Ag}^+$  solutions (Figure 3(b)). Clear comparable frequency shifts can be observed only after 30 minutes in low concentration. The obtained

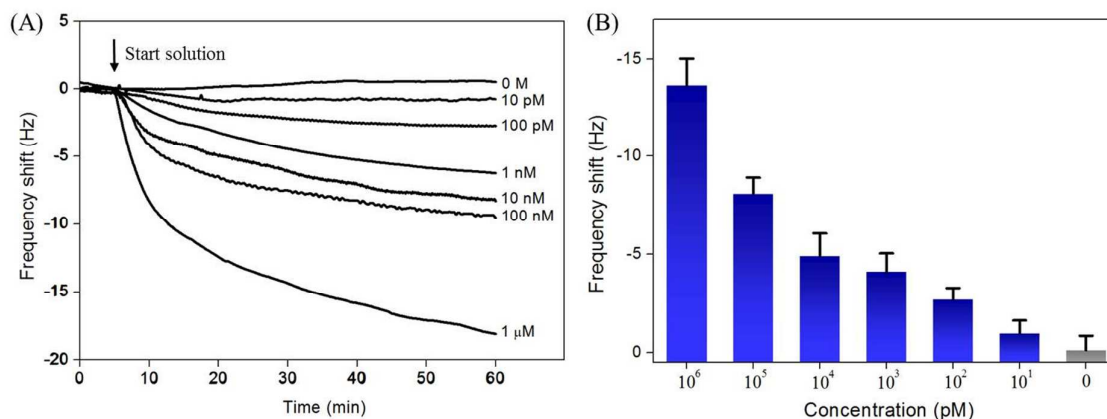


**Figure 3.**(A) In situ resonance frequency shift with respect to time at various Ag<sup>+</sup> ion concentrations. (B) Average resonance frequency shift after 30 min at different Ag<sup>+</sup> ion concentrations (blue bars) and control (gray bar). For the statistical data, we measured 5 different QCM data for each concentration. The error bar indicates the standard deviation.

frequency shift values of 1 μM, 100 nM, 10 nM, 1 nM, 100 pM, 10 pM and 0 M (control) Ag<sup>+</sup> solutions were 13.6 ± 1.4, 8.0 ± 0.8, 4.9 ± 1.2, 4.1 ± 0.9, 2.7 ± 0.6, 1.0 ± 0.7, and 0.1 ± 0.7 Hz, respectively. These results showed that the sensor was able to show the rapid response of frequency shift to a small Ag<sup>+</sup> concentration change with a high sensitivity. The difference in the average frequency shifts of 100 pM and the standard deviation value of the 0 M (control) was about 3.7 times, suggesting that the limit of detection (LOD) of our sensor was 100 pM. In case of limit of quantification (LOQ), LOQ was 1 nM in DI water. The reusability test was also performed using 1 μM of Ag<sup>+</sup> solution (Figure S3). Our purpose of reusability test is based on the high sensitive detection of Ag<sup>+</sup>. From this reason, we prepared reusability test using piranha solution which is also able to remove the probe DNA (c-DNA)<sup>34, 35, 36</sup>. The frequency shift for the first time use was 13.1 Hz. However, the frequency shift decreased to 11.2 Hz (twice), 7 Hz (3 times) and 6.4 Hz (4 times). Considering the detection performance for lower concentration and dramatic frequency shift decrease between twice and 3 times

**Table 1.** Characteristics of various sensor types for Ag ion detection with respect to detection limit, detection time, and label-free method availability (O: Label-free method, X: Labeled method).

Sensor type	Detection limit (nM)	Detection time (h)	Label-free method
QCM sensor (this work)	0.1	0.5	O
Graphene based fluorescent nanoprobe <sup>18</sup>	5	22	X
FRET sensor <sup>19</sup>	10	~ 3.8	O
Fluorescent (DNAzyme) sensor <sup>14</sup>	2.5	3	X
Gold nanoparticles colorimetric sensor <sup>15</sup>	52	12	O
	0.59	~ 0.5	X
Oscillator sensor <sup>17</sup>	1	26	O
KPFM sensor <sup>12</sup>	1	12	O

reuse, the electrode can be used for twice. We summarized the various sensor types of Ag<sup>+</sup> detection to emphasize advantages about our sensing platform. As shown in Table 1, QCM based sensor has the lowest limit of detection among the other types and also requires a very short detection time. Furthermore, it can directly detect Ag<sup>+</sup> by means of label-free.

The first derivative of the frequency shift of DI water with respect to time, denoted as F', was

also analyzed, as shown in Figure S4 (a). A sharp increase in the magnitude of  $F'$  was observed for 5 min after the exposure of the electrode to the  $\text{Ag}^+$  solutions, and an increase in the slope was also noticed with the increase in the  $\text{Ag}^+$  concentration. Therefore, we also summarized the slope of  $F'$  from DI water and drinking water with  $\text{Ag}^+$  concentration of  $10^6$ ,  $10^5$ ,  $10^4$ ,  $10^3$ ,  $10^2$  and 0 (Control), as shown in Figure S4 (b). We were able to observe that the overall slope of DI water was higher than in drinking water. The result implied that the reaction between  $\text{Ag}^+$  and nucleotides in DI water was faster than drinking water sample. In addition, the result also indicates that our sensor is capable of fast detection, which could be completed within 5 min, showing great potential for use as a direct monitoring tool.

We also examined the selective detection ability of this sensor by conducting experiments with a series of other metal ions representative in environment, including  $\text{Na}^+$ ,  $\text{Li}^+$ ,  $\text{Ca}^{2+}$ ,  $\text{Zn}^{2+}$ ,  $\text{Mg}^{2+}$  and  $\text{Fe}^{3+}$ . The concentration of these metal ions was fixed to 1  $\mu\text{M}$ . The obtained frequency shift values of  $\text{Na}^+$ ,  $\text{Li}^+$ ,  $\text{Ca}^{2+}$ ,  $\text{Zn}^{2+}$ ,  $\text{Mg}^{2+}$  and  $\text{Fe}^{3+}$  ions were  $2.3 \pm 8.9$ ,  $0.6 \pm 6.0$ ,  $1.6 \pm 3.2$ ,  $5.0 \pm 6.2$ ,  $2.3 \pm 1.7$ , and  $5.3 \pm 6.9\%$ , respectively. In the case of  $\text{Ag}^+$ , error bar was not shown because  $\text{Ag}^+$  was the base line. The frequency shift values of these ions were comparable to the result of 0 M (control)  $\text{Ag}^+$  and were negligibly small as compared with the result of 1  $\mu\text{M}$   $\text{Ag}^+$  (100 %) (Figure 4), indicating the superior selectivity of  $\text{Ag}^+$  detection of the technique. The selective detection of  $\text{Ag}^+$  was achieved by the single cytosine amplifier. The positively charged metal ions are known to interact with DNA on the negatively charged phosphates of the backbone and electron donor atoms from guanine and adenine<sup>37</sup>. When metal ion interact with DNA, mass increases as amount of adsorbed metal ion on DNA. However, when  $\text{Ag}^+$  interact with DNA, mass increases as amount of adsorbed  $\text{Ag}^+$  as well as single cytosine molecules which act as mass amplifier only for case of  $\text{Ag}^+$ .

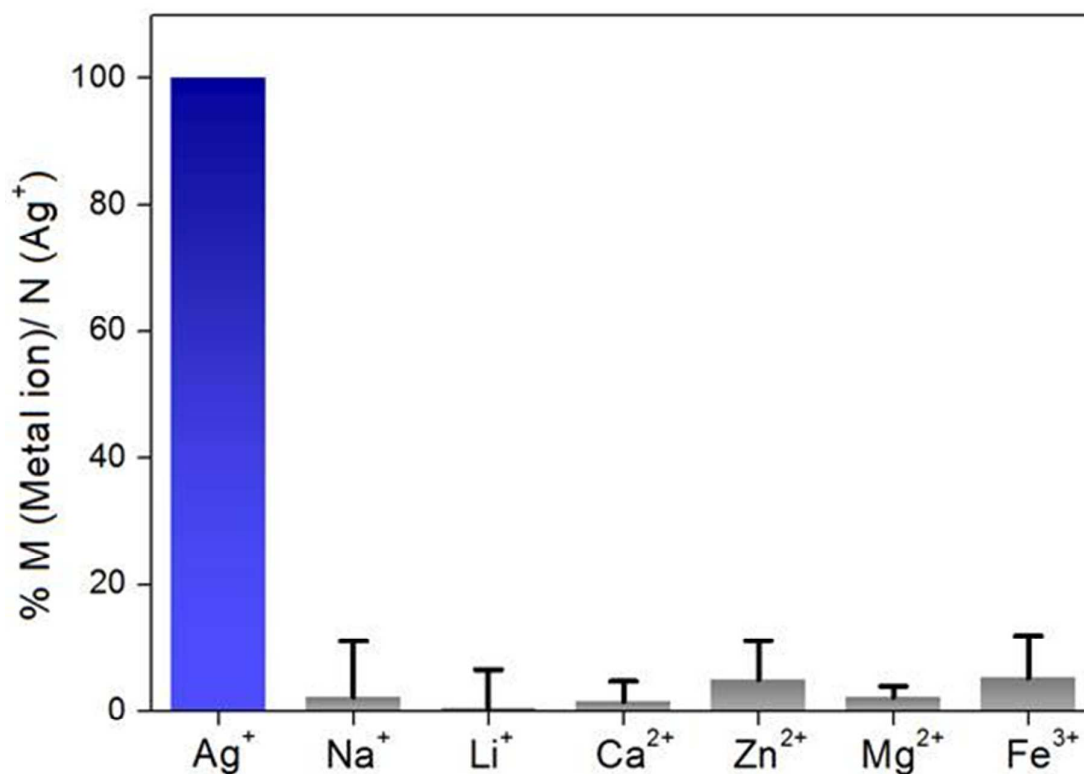


**Figure 4.** Analysis of Ag<sup>+</sup> ion selectivity of the method. The concentrations of Ag<sup>+</sup> ions (blue bar) and all other interfering metal ions (gray bars) were 1 μM. For the statistical data, we measured 5 different QCM data for each ion. The error bar indicates the standard deviation.

In order to evaluate the performance of the sensor for detecting real samples, we further performed experiments using commercially available drinking water (SamDaSoo, Kwangdong Corp., Korea). Figure 5(a) shows the detection results of Ag<sup>+</sup> ions in the drinking water sample. Similar to the frequency shift detected in DI water, the frequency shift in drinking water responded promptly to the change in the Ag<sup>+</sup> concentration. Furthermore, we analyzed the frequency shift in 1 h after the exposure of the electrode to Ag<sup>+</sup> (Figure 5(b)). The obtained frequency shift values were  $10.2 \pm 0.5$ ,  $6.0 \pm 1.5$ ,  $4.1 \pm 0.6$ ,  $2.6 \pm 0.4$ ,  $1.8 \pm 0.4$ , and  $0.5 \pm 0.5$  Hz at Ag<sup>+</sup> concentrations of 1 μM, 100 nM, 10 nM, 1 nM, 100 pM, and 0 M

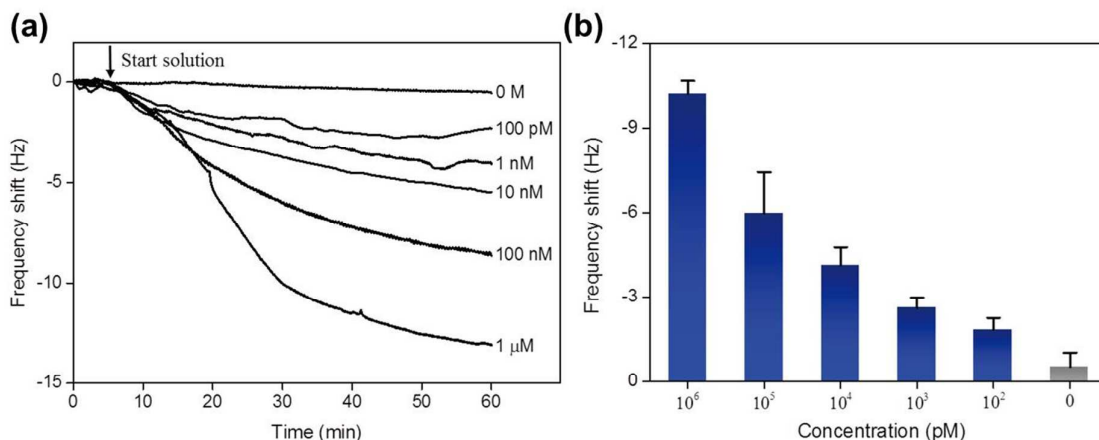


**Figure 5.** (A) In situ resonance frequency shift with respect to time at different Ag<sup>+</sup> ion concentrations in drinking water. (B) Average resonance frequency shift after 30 min at different Ag<sup>+</sup> ion concentrations (blue bars) and control experiment (gray bar) in drinking water. For the statistical data, we measured 5 different QCM data for each concentration. The error bar indicates the standard deviation.

(control), respectively. The overall frequency shift values in drinking water were lower than those obtained in DI water. It is attributed to the large amounts of interfering ions such as Ca<sup>2+</sup> (62.4 μM), K<sup>+</sup> (38.4 μM), Na<sup>+</sup> (174 μM), and Mg<sup>2+</sup> (69.9 μM), which coexisted with Ag<sup>+</sup> in the drinking water and interrupted the interaction of Ag<sup>+</sup> with cDNA and single cytosine. The selective detection was also performed in drinking water sample by adding 1 μM of Zn<sup>2+</sup>, Mg<sup>2+</sup>, so in drinking water experiment sample, total concentration of Zn<sup>2+</sup> ion was 1 μM and total concentration of Mg<sup>2+</sup> was expected to be 70.9 μM. The selective detection of Ag<sup>+</sup> was observed in drinking water (Figure S5) and the result implied that interfering ions interrupt the detection of Ag<sup>+</sup>, but the interruption did not attribute to the frequency shift. The LOD and LOQ for testing drinking water was 100 pM and 10 nM, which the values satisfying the sensitivity requirement (46 μM) for detecting standard drinking

water, as stipulated by the US Environmental Protection Agency (EPA).

#### 4. Conclusions

We have developed an ultra-sensitive QCM sensor for selective detection of  $\text{Ag}^+$  by using silver-specific DNAs in aqueous media. The effectiveness of using silver-specific DNAs was determined by a mass analysis using QCM. The sensor developed in this study showed good capability for capturing  $\text{Ag}^+$ , with the detection limit as low as 100 pM in DI water. The detection limit in the drinking water sample was also 100pM, which is still much lower than the standard stipulated by Environmental Protection Agency ( $< 46 \mu\text{M}$ ). In contrast to the conventional methods, this method is label-free and ultra-sensitive, capable of direct rapid detection and real-time monitoring. These advantages can largely reduce the detection costs and allow for the selective measurement of  $\text{Ag}^+$  among other interfering ions in drinking water, implying the feasibility of the method. Furthermore, the obtained results suggest the great promise of using QCM system for drinking water analysis and toxic metal ion detection due to its ultrahigh-sensitivity and selectivity. For future study, the damping of the QCM oscillation should be monitored in order to verify the confirmation of cytosine- $\text{Ag}^+$ -cytosine base pairs formation upon stiffness change and other parameters such as precision and robustness should be analyzed for the evaluation of detection performance.

#### 5. Acknowledgements

This study was supported by the National Research Foundation of Korea (NRF) under grant numbers of NRF-2012-0000785, NRF-2012-0006646, NRF-2014R1A2A1A11052389 and NRF-2013R1A1A1058102 funded by the Ministry of Science, ICT & Future Planning.

## References

1. J. S. Kim, E. Kuk, K. N. Yu, J.-H. Kim, S. J. Park, H. J. Lee, S. H. Kim, Y. K. Park, Y. H. Park, C.-Y. Hwang, Y.-K. Kim, Y.-S. Lee, D. H. Jeong and M.-H. Cho, *Nanomedicine: Nanotechnology, Biology and Medicine*, 2007, 3, 95-101.
2. V. K. M. Poon and A. Burd, *Burns*, 2004, 30, 140-147.
3. S. Siddhartha, B. Tanmay, R. Arnab, S. Gajendra, P. Ramachandrarao and D. Debabrata, *Nanotechnology*, 2007, 18, 225103.
4. C.-H. Liu and X. Yu, *Nanoscale Research Letters*, 2011, 6, 75.
5. K.-Y. Chun, Y. Oh, J. Rho, J.-H. Ahn, Y.-J. Kim, H. R. Choi and S. Baik, *Nat Nano*, 2010, 5, 853-857.
6. H. T. Ratte, *Environmental Toxicology and Chemistry*, 1999, 18, 89-108.
7. H. C. Fischer and W. C. W. Chan, *Current Opinion in Biotechnology*, 2007, 18, 565-571.
8. C. Beer, R. Foldbjerg, Y. Hayashi, D. S. Sutherland and H. Autrup, *Toxicology Letters*, 2012, 208, 286-292.
9. M. Rahban, A. Divsalar, A. A. Saboury and A. Golestani, *The Journal of Physical Chemistry C*, 2010, 114, 5798-5803.
10. G. J. Ramelow, R. S. Maples, R. L. Thompson, C. S. Mueller, C. Webre and J. N. Beck, *Environmental Pollution*, 1987, 43, 247-261.
11. G. Cabana and J. B. Rasmussen, *Nature*, 1994, 372, 255-257.
12. J. Park, S. Lee, K. Jang and S. Na, *Biosensors and Bioelectronics*, 2014, 60, 299-304.
13. N. Zimmermann, E. Meggers and P. G. Schultz, *Journal of the American Chemical Society*, 2002, 124, 13684-13685.
14. T. Li, L. Shi, E. Wang and S. Dong, *Chemistry – A European Journal*, 2009, 15, 3347-3350.
15. B. Li, Y. Du and S. Dong, *Analytica Chimica Acta*, 2009, 644, 78-82.
16. A. Ono, S. Cao, H. Togashi, M. Tashiro, T. Fujimoto, T. Machinami, S. Oda, Y. Miyake, I. Okamoto and Y. Tanaka, *Chemical Communications*, 2008, 0, 4825-4827.
17. J. Park, W. Choi, K. Jang and S. Na, *Biosensors and Bioelectronics*, 2013, 41, 471-476.
18. Y. Wen, F. Xing, S. He, S. Song, L. Wang, Y. Long, D. Li and C. Fan, *Chemical Communications*, 2010, 46, 2596-2598.
19. A. Ono, S. Cao, H. Togashi, M. Tashiro, T. Fujimoto, T. Machinami, S. Oda, Y. Miyake, I. Okamoto and Y. Tanaka, *Chemical Communications*, 2008, 4825-4827.
20. G. Sauerbrey, *Z. Physik*, 1959, 155, 206-222.
21. R. Schumacher, *Angewandte Chemie International Edition in English*, 1990, 29, 329-343.
22. M. Rodahl, F. Höök and B. Kasemo, *Analytical Chemistry*, 1996, 68, 2219-2227.
23. L. Baldini, M. Melegari, V. Bagnacani, A. Casnati, E. Dalcanale, F. Sansone and R. Ungaro, *The Journal of Organic Chemistry*, 2011, 76, 3720-3732.

24. K. Feng, J. Li, J.-H. Jiang, G.-L. Shen and R.-Q. Yu, *Biosensors and Bioelectronics*, 2007, 22, 1651-1657.
25. R. Hao, D. Wang, X. e. Zhang, G. Zuo, H. Wei, R. Yang, Z. Zhang, Z. Cheng, Y. Guo, Z. Cui and Y. Zhou, *Biosensors and Bioelectronics*, 2009, 24, 1330-1335.
26. L. Qingwen, G. Hong, W. Yiming, L. Guoan and M. Jie, *Electroanalysis*, 2001, 13, 1342-1346.
27. Q. Chen, X. Wu, D. Wang, W. Tang, N. Li and F. Liu, *Analyst*, 2011, 136, 2572-2577.
28. H. Ogi, T. Yanagida, M. Hirao and M. Nishiyama, *Biosensors and Bioelectronics*, 2011, 26, 4819-4822.
29. L. B. Nie, Y. Yang, S. Li and N. Y. He, *Nanotechnology*, 2007, 18, 305501.
30. W. Tang, D. Wang, Y. Xu, N. Li and F. Liu, *Chemical Communications*, 2012, 48, 6678-6680.
31. K. Jang, J. Park, D. Bang, S. Lee, J. You, S. Haam and S. Na, *Chemical Communications*, 2013, 49, 8635-8637.
32. J. You, K. Jang, S. Lee, D. Bang, S. Haam, C.-H. Choi, J. Park and S. Na, *Biosensors and Bioelectronics*, 2015, 68, 481-486.
33. C. Zhao, K. Qu, Y. Song, C. Xu, J. Ren and X. Qu, *Chemistry – A European Journal*, 2010, 16, 8147-8154.
34. Y. Zhang, H. Wang, B. Yan, Y. Zhang, J. Li, G. Shen, and R. Yu, *Journal of Immunological Methods*, 332, 103-111
35. L. Loo, W. Wu, W. Shih, W. Shih, H. Borghaei, K. Pourrezaei, and G. Adams, *Sensors*, 11, 5520.
36. K. Fumihito, O. Hirotsugu, Y. Taiji, N. Shintaro, N. Masayoshi, and H. Masahiko, *Japanese Journal of Applied Physics*, 50, 07HD03
37. J. Anastassopoulou, *Journal of Molecular Structure*, 2003, 651-653, 19-26.